Studying Two-Dimensional Systems with the Density Matrix Renormalization Group

E.M. Stoudenmire and Steven R. White

Department of Physics and Astronomy, University of California, Irvine, Irvine, California 92697; email: estouden@uci.edu, srwhite@uci.edu

Annu. Rev. Condens. Matter Phys. 2012. 3:111–28

First published online as a Review in Advance on December 14, 2011

The *Annual Review of Condensed Matter Physics* is online at conmatphys.annualreviews.org

This article's doi: 10.1146/annurev-conmatphys-020911-125018

1947-5454/12/0310-0111$20.00

Keywords

strongly correlated electrons, frustrated magnetism, computational/numerical methods, tensor product wavefunctions

Abstract

The density matrix renormalization group (DMRG) is one of the most powerful numerical methods for studying two-dimensional quantum lattice systems, despite a perception that it is only suitable for one dimension. Reviewing past applications of DMRG in 2D demonstrates its success in treating a wide variety of problems, although it remains underutilized in this context. We present techniques for performing cutting-edge 2D DMRG studies including methods for ensuring convergence, extrapolating finite-size data, and extracting gaps and excited states. Finally, we consider a selection of recently developed 2D tensor network methods and compare the performance of one of these to 2D DMRG.

1. INTRODUCTION

The behavior of quantum many-body lattice systems depends strongly on their dimensionality. Mean-field theory—where the behavior at each site is determined self-consistently by the average influence of all its neighbors—works best when there are many neighbors, that is, in higher dimensions. Three-dimensional systems can often be well understood using mean-field or semiclassical approaches, with quantum fluctuations acting as a minor correction (1, 2). In one dimension, mean-field theory usually fails, and exotic behavior driven by strong quantum fluctuations, such as spin-charge separation, is the norm. By using powerful analytical and numerical approaches developed over the past few decades, it is possible to determine the properties of 1D systems to high accuracy.

Two-dimensional systems often have substantial quantum fluctuations, causing mean-field approaches to fail. Yet geometrical constraints are much more relaxed than in 1D, allowing many more phases to exist. In some ways, geometry specifically selects 2D as being the most interesting: For example, in 2D a pair of particles can circle one another, unlike in 1D; but different numbers of revolutions (and their signs) are topologically distinct, unlike in three or more dimensions. Thus it is possible—in 2D alone—for the elementary excitations of a system's ground state to be anyons, particles that are neither bosons nor fermions. Currently, two-dimensional systems are at the heart of quantum condensed matter physics, with a large fraction of researchers focusing their efforts on key families of two-dimensional systems, including the high-temperature superconducting cuprates (3, 4), quantum Hall systems (5), and frustrated magnets, especially those that could host spin liquids (6–9).

Most of the analytical and numerical techniques that often work in one or three dimensions fail in 2D. For example, analytic techniques based on the Bethe ansatz (an exact wavefunction for certain 1D systems) or on conformal field theory are specific to 1D (10). Another example is quantum Monte Carlo, one of the most powerful numerical methods (11, 12). Classical Monte Carlo methods work in any dimension, but the path-integral formulation needed for quantum Monte Carlo introduces probabilities that can be negative; this is known as the sign problem (13, 14). Quantum Monte Carlo is of limited usefulness for systems with a sign problem. Although the presence of the sign problem does not correspond strictly to dimensionality, 1D systems with nearest-neighbor interactions do not have a sign problem, whereas 2D or 3D systems with either mobile fermions or frustrating spin interactions do have a sign problem. Solving the sign problem is sometimes called one of the great challenges of condensed matter physics. Narrowly, solving the sign problem means fixing quantum Monte Carlo methods in some way, but we can also take a broader view: Can we find any numerical method that can solve broad classes of frustrated or fermionic quantum systems in 2D or 3D?

The density matrix renormalization group (DMRG) is a numerical approach designed for one dimension, which has become the most powerful known numerical method in 1D (15, 16). The subject of this review is the application of DMRG to 2D. It is more difficult to use DMRG in 2D, and the results are much less accurate than in 1D. Nevertheless, the lack of alternative approaches (when there is a sign problem) makes DMRG one of the most powerful current methods for certain 2D systems. It is a key goal of this review to present the tricks and techniques that are essential for the efficient treatment of 2D systems.

Unfortunately, DMRG has been underutilized in this context. One reason may be the idea that DMRG is not useful since it requires a computational effort scaling exponentially with the width of the system. However, this same argument would imply that exact diagonalization (solving for the ground state eigenvector utilizing the complete Hilbert space of a finite cluster) would not be useful even in 1D! In fact, exact diagonalization is often useful even in 2D

(17, 18). The exponential scaling of DMRG in 2D depends only upon the width, not the total number of sites as in exact diagonalization, and one often finds a fairly modest coefficient governing the exponential. Even in sign-problem-free models, DMRG can make predictions of similar quality to Quantum Monte Carlo (19).

Figure 1 shows two examples of results from recent 2D DMRG calculations. The system widths shown are close to the state of the art in terms of maximum system sizes reachable; but

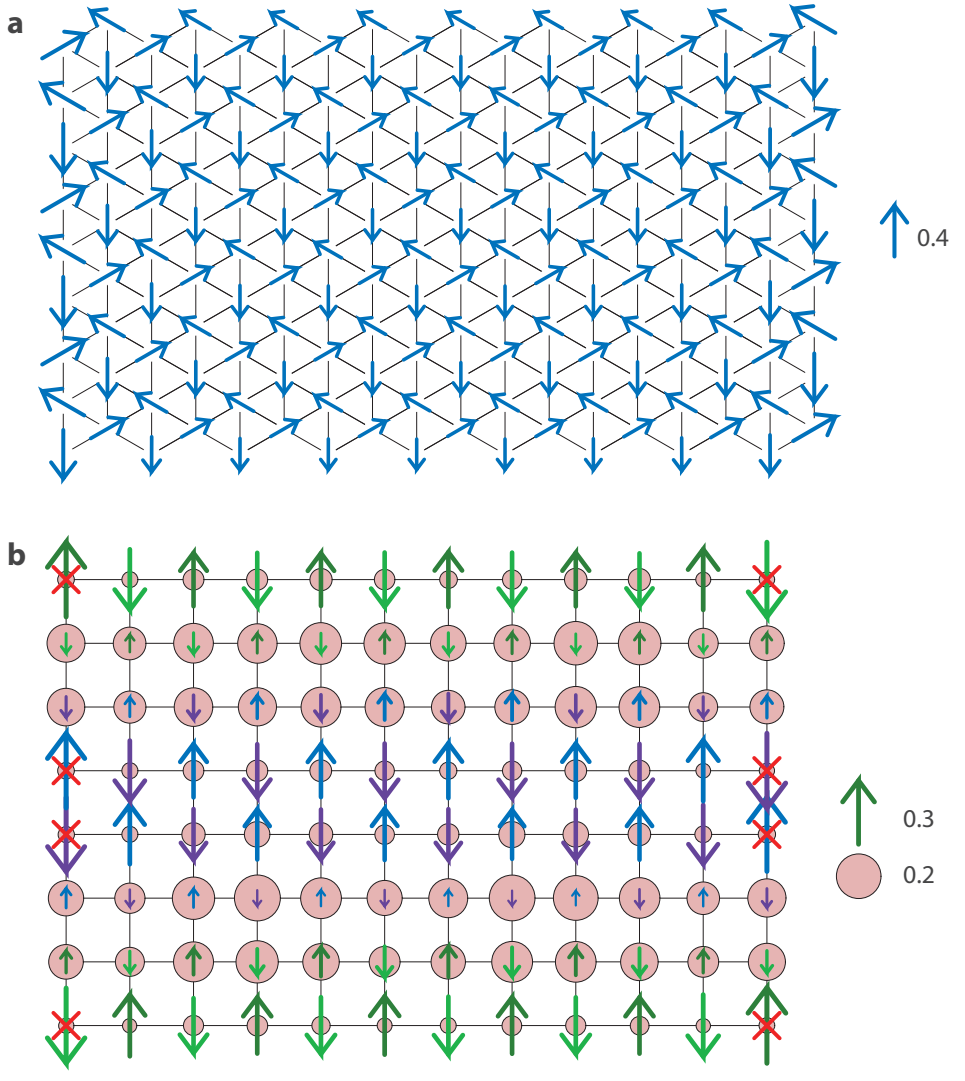

Figure 1

Results of density matrix renormalization group simulations on 2D systems with either frustration or mobile fermions. (*a*) Local values of $\langle \vec{S} \rangle$ for a triangular Heisenberg model. The 120° antiferromagnetic order is pinned by applied magnetic fields on the left and right edges; the top and bottom edges are connected to make a cylindrical geometry. (*b*) Spin and hole densities for a *t-J* cluster, which exhibits both stripes and pairing. Cylindrical boundary conditions are used, and pinning with both magnetic and proximity effect pair fields are used on the left and right open ends.

using the techniques discussed below in Section 3, it is often possible to extrapolate such DMRG results to the infinite 2D limit quite reliably. DMRG makes up for its size limitations even further by providing access to the entire many-body wavefunction, making it possible to compute essentially any ground state observable.

To understand how DMRG works, observe that although exact diagonalization describes the wavefunction in a complete, exponentially large basis, some of these coefficients and basis functions are much more significant than others. The idea of making a systematic approximation by truncating this basis is quite old, but in its simplest form it is not very effective for strongly correlated systems. In DMRG, one first rotates the basis so as to make the truncation much more accurate—in the rotated basis, only a few of the states are needed to represent the ground state, and the rest can be discarded. A rotation involving the whole Hilbert space would be inefficient; instead, DMRG uses many rotations focused on a few sites at a time, generating global rotations via a sweeping procedure through all the sites of the lattice. The result is a wavefunction written in a particular form, called a matrix product state or MPS. An alternative viewpoint for DMRG is to start with the MPS form as a variational ansatz, then optimize all its coefficients. From this viewpoint, DMRG is an extremely efficient method for optimizing the coefficients (15, 20). The basis used by DMRG is the optimal basis within a certain framework (21); in recent years it has been understood to be a straightforward consequence of the Schmidt decomposition of quantum information.

Because DMRG is so efficient, it has dominated numerical research in the subfield of strongly correlated 1D systems. One of the first applications of DMRG was calculating the excitation gap in the $S = 1$ Heisenberg chain to very high accuracy at a time when its existence remained controversial (22). Since then, not only has the original DMRG algorithm improved but its flexibility has allowed many extensions. For example, DMRG is very useful for studying time-dependent Hamiltonians (23) and finite-temperature systems (24, 25). Following the realization that DMRG is actually based upon MPS (26), the method has become highly influential within the quantum information community, leading to the development of a new breed of algorithms based on tensor network states (27–29). These developments have in turn accelerated the power and flexibility of the original DMRG method. For example, it is now possible to use DMRG to reliably determine the ground state of infinite 1D systems (30).

Although the hope is that tensor network state approaches will eventually overtake DMRG in two-dimensional studies (see Section 4), in the meantime it remains one of the most powerful and well-controlled methods for simulating models with a sign problem. DMRG can even be useful for simulating sign-problem-free models, given that it provides full access to the many-body wavefunction (31).

In the following section we review past applications of DMRG to 2D systems. In Section 3—a discussion of techniques for 2D—we assume a working knowledge of DMRG for 1D systems; for a detailed introduction see, for example, Schollwöck (20, 32), Hallberg (33), Noack & Manmana (34), and White (16).

2. APPLICATIONS OF THE TWO-DIMENSIONAL DENSITY MATRIX RENORMALIZATION GROUP

DMRG has been successfully used to study a wide variety of 2D systems—a testament to the flexibility of the method. We briefly survey some prior studies below, focusing especially on those that break new ground by introducing techniques or characterizing especially interesting systems. The hope is to convey an understanding of what is possible with current methods and to motivate the investigation of systems that are good candidates for a DMRG study.

One of the first applications of DMRG was in the area of magnetism (22). Magnetic models, such as the Heisenberg model, are ideally suited for DMRG because they can exhibit interesting phases with only modest entanglement and rarely suffer from large differences in energy scales. Among the first 2D magnetic models to be studied with DMRG was the frustrated $S = 1/2$ Heisenberg antiferromagnet on the CAVO lattice (35). This study helped establish the usefulness of DMRG for 2D systems and introduced the wavefunction acceleration technique, improving performance by up to two orders of magnitude. Since then, 2D DMRG has been used to study the frustrated nearest-neighbor Heisenberg model on the triangular (19, 36, 37) and kagome (9, 38) lattices as well as models frustrated by further-neighbor or multispin interactions (39–43). Two-dimensional DMRG is powerful enough to be a good option for studying unfrustrated spin models too (44–46). One recent study obtained an estimate for the magnetization of the square lattice Heisenberg model competitive with the best published Quantum Monte Carlo results (19).

An area where 2D DMRG has been especially fruitful is in the search for quantum spin liquids—magnetic systems that break no symmetries down to $T = 0$. Many realistic, one-dimensional spin models have disordered ground states, but the search for realistic 2D spin liquids remains a challenge (6). To date, DMRG has been used to identify two-dimensional spin liquid phases stabilized by anisotropic (37, 44), further-neighbor (39, 40) and multispin (41, 42) interactions, yet definitive evidence of a short-range, isotropic spin model whose ground state breaks no symmetries has been lacking. However, DMRG simulations of the Heisenberg antiferromagnet on the kagome lattice now show strong evidence for a spin liquid ground state (9). 2D DMRG has also been used recently to study perturbations to the unrealistic Kitaev honeycomb model that may actually describe a certain limit of the layered magnet Na_2IrO_3 (43).

Another set of systems studied extensively with 2D DMRG is the doped *t-J* and Hubbard models. DMRG is an attractive option for simulating models of this type because it can deal with arbitrary doping in an unbiased way. A common thread in the DMRG literature on the *t-J* and Hubbard models is the formation of stripes—charge density waves separating regions of phase-shifted antiferromagnetic order. After stripes were found to occur spontaneously in four-leg *t-J* ladders (47), they were also found to occur in systems up to width eight (48). Follow-up studies have examined properties of stripes more closely, such as their doping and interaction energy (49) and the effects of further-neighbor interactions (50, 51) and anisotropies (52) likely present in real materials. It was suggested early on that the stripes observed experimentally are due to frustrated phase separation (53), but evidence from DMRG favors the idea that stripes are caused by local competition between hopping and exchange, without the need for long-range Coulomb interactions (54). Two-dimensional DMRG results may also shed light on the pairing mechanism of the cuprates (55).

One study that especially highlighted the reliability of DMRG results for 2D *t-J* models was Chernyshev et al.'s (56, 57) comparison of 2D DMRG results to predictions from a self-consistent Green function theory of holes in an antiferromagnetic background. Working with a modified *t-J* model where J is replaced by an Ising J_z interaction, the two methods show remarkable correspondence in their predictions of energies and hole distributions, especially for the case of a single hole (56, 57). Further DMRG investigations of the *t-J* model have examined the existence of checkerboard order (58), edge states of holes in nanosystems (59), and the competition between stripes and pairing (60). DMRG has also been used to demonstrate a striped phase in the Hubbard model on systems up to width six (61–63).

Another class of systems well suited for 2D DMRG is frustrated bosonic models, although there have been few DMRG studies of these systems until very recently. Bosonic models can be simple to work with numerically, yet are expected to exhibit new kinds of phases and exotic

orders not found in one dimension. They also have great potential for controlled experimental realizations with cold atoms. One topic in bosonic systems that has attracted great interest is the possibility of a supersolid, a phase with simultaneous charge density wave and superfluid order. A supersolid phase was shown to exist in the unfrustrated triangular lattice model, but the order turned out to be quite weak. However, using 2D DMRG, Jiang et al. (64) have demonstrated that adding further-neighbor hopping to the model significantly stabilizes supersolid order.

A rather different kind of bosonic phase predicted to exist in 2D is known as a bose metal. This phase is not captured by a conventional order parameter, but instead by a pattern of correlations associated with an entire surface of gapless modes (a bose surface) (65). Using DMRG, it has proved possible to identify remnants of the full 2D surface in quasi-1D models with ring-exchange interactions on two-leg (41, 66) and four-leg (42) ladders. A related work explores a novel gapped phase of bosons on three-leg ladders (67). Motivated by the original construction of the bose metal in terms of fermionic partons, DMRG calculations have also been used to show that a frustrated 2D fermionic model could enter a Cooper-pair bose metal phase (68). Recently, a rather different type of ordering was observed for a fermionic system on the kagome lattice, where 2D DMRG was used to study a metal-insulator transition (69).

One final study that does not fit neatly into the above categories but certainly bears mentioning is the investigation by Jeckelmann & White (70) of the Holstein model, which describes a single fermion interacting with bosonic lattice vibrations or phonons. An effective way of dealing with the large number of boson species in this model was to split each site into many smaller ones having fewer degrees of freedom. Using this technique, it proved possible to simulate cylindrical systems with widths up to 20!

3. TECHNIQUES FOR THE TWO-DIMENSIONAL DENSITY MATRIX RENORMALIZATION GROUP

When working at the frontier of current numerical capabilities, it is important to ensure that individual simulations give trustworthy results and then combine these results correctly to build an accurate picture of a 2D model. For two-dimensional DMRG, the main obstacle to overcome is that the number of states kept must be increased exponentially with the width of the system to maintain a constant accuracy (71). In practice, this puts an upper bound on the system sizes that can be simulated. In addition, one should use open or cylindrical boundary conditions, as opposed to fully periodic boundary conditions, to avoid squaring the number of states required for a given accuracy (see below).

Although the first restriction is unfortunate, the use of cylindrical boundary conditions is hardly the drawback it is often portrayed to be. In fact, cylindrical boundaries provide a significant degree of control over simulations and can be very useful for inferring properties of the full 2D system. The limitations of two-dimensional DMRG are further mitigated by the enormous flexibility of the DMRG approach. DMRG gives full access to the many-body wavefunction. This means, for instance, that the ground state computed for one Hamiltonian can be used as input for simulations with a different Hamiltonian, inviting a range of techniques such as biasing initial states to detect symmetry breaking or changing a Hamiltonian in midsimulation to locate phase boundaries.

In what follows we discuss these techniques and others that have been successfully used in cutting-edge calculations. The hope is to equip practitioners to pursue new state-of-the-art 2D DMRG calculations and to motivate them to create their own techniques, extending the reach of current numerical methods.

3.1. Ensuring Ground State Convergence

A successful DMRG study of a two-dimensional system involves multiple independent calculations for various system sizes over a range of parameters. To deduce the correct behavior of the 2D system from these results, one must guarantee that each ground state calculation is well understood and as accurate as possible. DMRG can fail to find the true ground state for two basic reasons. The first is that the number of states kept after each truncation of the wavefunction may be too small to represent the wavefunction accurately. The second issue is more subtle and arises because although DMRG uses exact diagonalization locally, it is globally a variational method and can therefore get stuck in a metastable state (72).

There are several ways to ensure that one does not over-truncate the wavefunction and that a sufficient number of states m are being kept. Most important is to avoid using fully periodic boundary conditions, as they require m^2 states to represent the same wavefunction requiring only m states with open or cylindrical boundary conditions (32). By cylindrical boundary conditions we mean open boundary conditions along the larger lattice direction (the length, or x direction) and periodic boundary conditions along the smaller direction (the width). A typical setup using cylindrical boundary conditions is shown in **Figure 2**.

After a calculation is under way, the number of states kept should be increased systematically until the energy and any other observables of interest converge to a specified tolerance. This can be done by directly adjusting m, or by fixing the maximum truncation error at a step and having the code determine m on the fly. An optimal approach may involve taking both a maximum (and minimum) m into account as well as a requested truncation error. A minimum m is important because the reported truncation error early on in the calculation could be inaccurate, resulting in slow convergence because of too small an m.

Metastability issues are more difficult to deal with systematically. Practitioners must use several checks in addition to physical insight to verify that the wavefunction has reached the true ground state. For many models, specific properties of the ground state are known in advance. Additionally, if one uses a DMRG code that represents wavefunctions as an MPS, then by representing the Hamiltonian as a matrix product operator it is possible to efficiently compute the variance $\sigma_H = \langle\psi|H^2|\psi\rangle - E_\psi^2$ and confirm that $|\psi\rangle$ is an eigenstate.

There is a general technique that helps DMRG avoid being stuck in metastable states. This technique is particularly helpful in making sure the MPS wavefunction includes correlations coming from terms in the Hamiltonian connecting distant sites in the MPS path. For example, a nearest-neighbor hopping in a 2D strip may connect sites that are the transverse width apart in the MPS path. These correlations may have trouble getting started, given that the extra states needed to allow the hopping at one of the two sites may not help lower the energy unless the

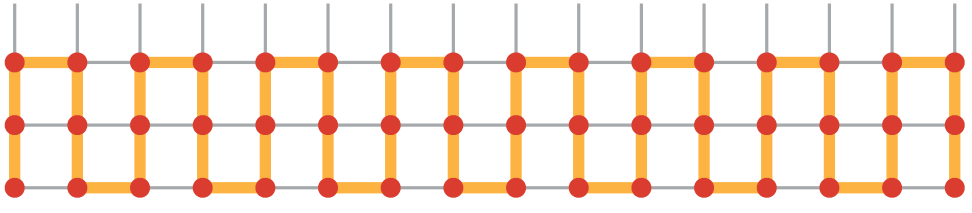

Figure 2

Interaction bonds for a nearest-neighbor model with cylindrical boundary conditions on a three-leg ladder. The thicker bonds (orange) indicate interactions that remain nearest neighbor along the 1D path used by the density matrix renormalization group, whereas thinner bonds (gray) are treated as further-neighbor interactions.

extra states at the other site are already present. A special noise term can be added to the density matrix at each step that takes into account all terms connecting the left and right blocks (73). This extra noise helps such long-range correlations get started; generally, the noise is turned off in later sweeps. This technique is particularly important if, for some reason, fully periodic boundary conditions must be used.

A key way to avoid metastability is to begin with a wavefunction that is already close to the true ground state. Good initial wavefunctions may be hard to come by for an unfamiliar model; here, careful calculations on smaller system sizes or at smaller values of m where DMRG has better control can be an excellent guide. Such calculations allow one to identify the dominant correlations within the ground state that may otherwise be obscured by strong fluctuations on larger lattices or for larger m.

For a system that is expected to have a conventional symmetry-breaking ground state, such as an antiferromagnet on a bipartite lattice, a Néel state may be a sufficiently good starting point. For systems with more subtle order, the initial wavefunction can be produced by starting with a lower symmetry or pinned Hamiltonian. For example, if a system is expected to have a ground state with valence-bond-solid order, the Hamiltonian can be modified by adding pinning fields $\lambda \vec{S}_i \cdot \vec{S}_j$ for each pair of sites i, j connected by a valence bond. Then, after a few sweeps, λ can be gradually tuned to zero, allowing the system to relax to its true ground state.

Using an initial state or a pinning field can also be helpful for ruling out hypothesized properties of a model. If DMRG restores a symmetry explicitly broken by the initial state, one has strong evidence against that particular ordering scenario. This method has been used to rule out a type of checkerboard order for the *t-J* model (58) and more recently as evidence against a particular type of valence-bond-solid order for the kagome Heisenberg antiferromagnet (9).

When dealing with a complex lattice or a phase with a large unit cell, one way to deal with metastability issues and minimize the number of states needed is to experiment with multiple DMRG paths. For a fixed value of m, DMRG is better able to capture entanglement on Hamiltonian bonds that remain nearest neighbor when mapped to 1D. Choosing the DMRG path judiciously can even permit complex initial wavefunctions such as valence-bond solids to be represented exactly with only a small value of m. Having the ability to reproduce the same ground state with different DMRG paths can also provide strong evidence that one has found the true ground state and not a metastable solution.

After having gained a good understanding of smaller systems, one wants to push DMRG calculations up to the largest accessible widths. At these widths, there is less control, so to produce accurate results it is useful to extrapolate from more controlled limits. For DMRG, a natural extrapolation parameter is the truncation error ε (the sum of discarded density matrix eigenvalues). The energy has long been extrapolated to zero truncation error, where normally a linear extrapolation of E versus ε is best. Remarkably, within a DMRG calculation local measurements performed on the two central sites at each step also have errors varying linearly with ε! This is one reason why measuring local quantities, perhaps in response to a perturbation, is usually preferred to correlation functions, whose error varies as $\varepsilon^{1/2}$ (19). Efficient extrapolations can be performed using results from a single DMRG calculation with increasing m, but it is important to repeat each m for two full sweeps (and to extrapolate using the last of the four half-sweeps) to ensure that the calculated ε is consistent enough for extrapolation.

The flexibility of DMRG even allows the use of other extrapolation parameters that may work better than the truncation error in certain cases. For example, one can add a small perturbation $\lambda H'$ to the Hamiltonian and extrapolate the energy in λ. For this approach to work well, the ground states of the perturbed Hamiltonian should be less entangled than the true ground state. Furthermore, by choosing H' to have a vanishing expectation value with

respect to the ground state of H, the first derivative of the energy with λ can be tuned to zero, increasing the accuracy of the extrapolation (9).

3.2. Working Around Finite-Size Limitations

A variety of approaches can be taken to predict bulk 2D behavior from sets of finite systems; here we discuss some that are particularly useful in the context of DMRG. Most of these approaches utilize cylindrical boundaries. On the two open edges of the cylinder, one is free to apply local fields (pinning it), or to perturb it in other ways, to make the bulk represent 2D most accurately. A favorable side effect of applying a boundary pinning field may be a reduction of entanglement, improving the DMRG convergence. For example, an antiferromagnet on a finite system typically has a singlet ground state, but one may regard it as a superposition of antiferromagnetically ordered states with different directions for the order parameter. Pinning can select one order parameter direction, reducing the complexity and entanglement of the state, while simultaneously representing the broken-symmetry 2D properties more faithfully (19).

It is useful to choose strongly pinned edges. To choose this type of pinning, it is helpful to think of the finite cylindrical system as part of an infinite cylinder. A fictitious infinitely strong pinning field is applied to the fictitious system outside the finite part. The fictitious part then acts on the boundary of the real system through the Hamiltonian terms connecting the two. **Figure 3** shows the results of a ground state calculation for the $S = 1/2$ Heisenberg model on a cylinder of width 8 and length 16. Two rows of the fictitious system are also shown at each end of the cylinder. The magnetization is enhanced near the pinned sites then approaches the 2D bulk value at the center (if the aspect ratio is chosen properly as discussed below).

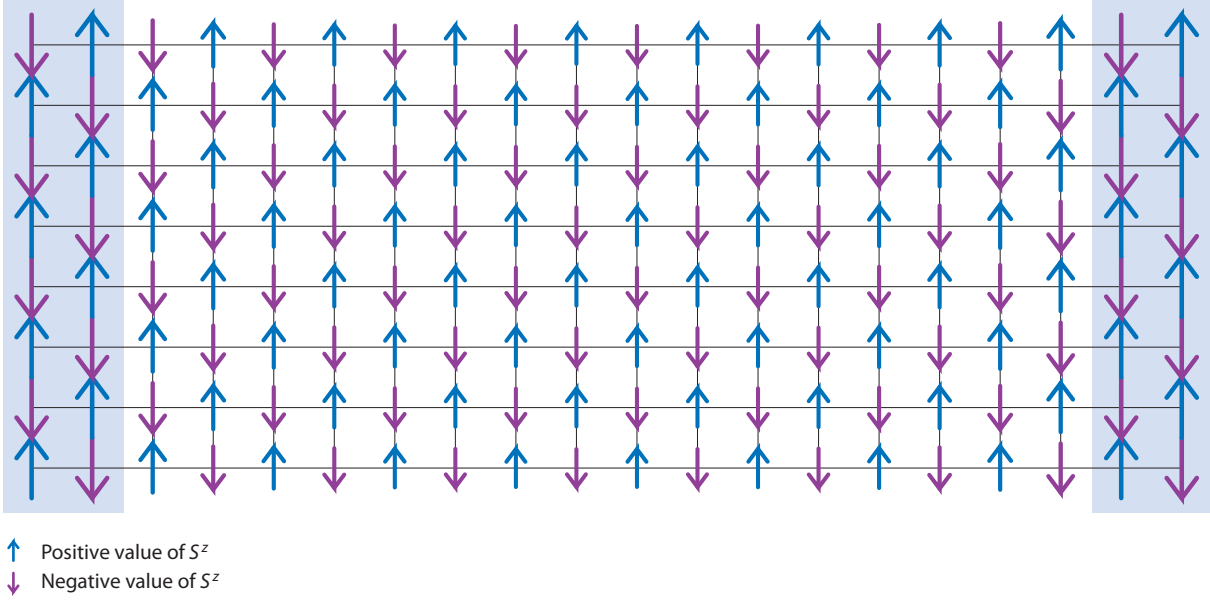

Figure 3

Results of a density matrix renormalization group calculation for the Heisenberg model on a 16 × 8 cylinder with antiferromagnetic order pinned at the open boundaries. To work in the strong pinning limit, it is useful to imagine the finite system embedded within a larger system acted on by an infinitely strong field (*light blue shaded regions*). The pinning fields at the physical edges are determined by the Hamiltonian bonds connecting the real and fictitious system.

After gaining a good understanding of the system's ground state properties, the next step is to simulate multiple system sizes to build up an accurate picture of the thermodynamic limit. Because DMRG scales much more favorably with the length of a system than with its width, it is a good idea to group results together for a given fixed width. Naively then, it would seem that the best approach is to simulate the longest possible system at each width. But there are much more efficient ways to proceed.

For a fixed width, the energy per site of a length L_x system approaches the infinite system value with an error proportional to $1/L_x$ because of a constant term in the energy from the open ends. This slow convergence reduces the efficiency and accuracy of direct extrapolations. Therefore, it is convenient to determine bulk cylinder energies by subtracting the energies of different finite-length cylinders. As illustrated in **Figure 4**, subtracting cancels edge effects, leaving only the bulk energy of the larger system, which rapidly converges to the infinite value as a function of L_x. The convergence rate depends on the bulk correlation length(s). If the correlation lengths are infinite, one can extrapolate the subtracted energies with a polynomial for the highest accuracy.

As an example of the subtraction method, **Figure 5** shows results for the square lattice $S = 1/2$ Heisenberg model on six leg ladders of length $L_x = 8$ through $L_x = 20$. The bare energies of the finite ladders have a strong $1/L_x$ dependence, but the subtracted energies rapidly converge to a constant value and require no fine tuning of the boundary conditions. Although one has to extrapolate the single-cylinder data, the subtracted energies converge quickly enough that the best point can be used as the infinite cylinder energy estimate.

Finally, after obtaining the bulk energies of infinite cylinders with various widths L_y, one can extrapolate in L_y to estimate the 2D energy. For the case of periodic boundary conditions—applicable for the infinite cylinders—the leading finite-size corrections to the energy density of the Heisenberg model are expected to vary as $1/L_y^3$ (74). In **Figure 6** we show the result of fitting the infinite cylinder energies with $L_y \geq 6$ to this form. We obtain an estimate $\varepsilon_0 = -0.6694(3)$ consistent with the best published Monte Carlo result $\varepsilon_0 = -0.669437(5)$ (75).

Bulk order parameters should be obtained differently from energies—considering infinite cylinders is not optimal. Asymptotically, infinite length cylinders of constant width will exhibit 1D behavior.

A particularly effective approach for measuring order parameters is to try to choose an optimal aspect ratio $\alpha = L_x/L_y$ for finite cylinders. The approach utilizes the strongly pinned boundary conditions described above. Say we decide to extrapolate to 2D only using cylinders with a fixed α. As illustrated in **Figure 7**, if α is too small, edge effects suppress fluctuations and our estimates approach the 2D value from above; if α is too large the physics resembles that of a 1D chain and our estimates approach from below. In several typical systems and in associated continuum theories it has been found that there is an optimal ratio α^* where leading corrections

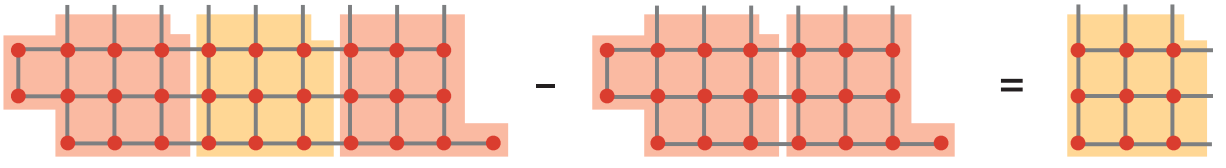

Figure 4

Properties at open edges are not typical of the bulk model and may include pinning fields or extra sites designed to accommodate a certain ground state. Subtracting energies calculated for two finite length systems cancels the leading edge effects, giving values that rapidly converge to the properties of the infinite cylinder.

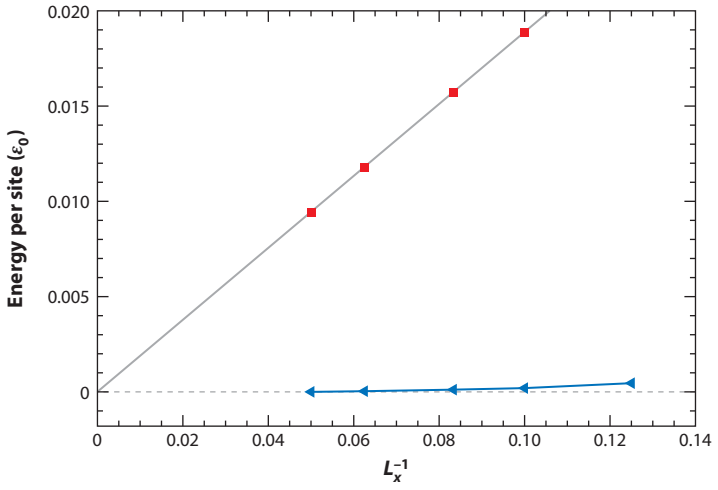

Figure 5

Subtraction method for estimating the energy per site of the $S = 1/2$ Heisenberg model on an infinite cylinder of width $L_y = 6$. The upper points (*red squares*) are the energy per site of finite systems with $L_x =$ 10, 12, 16, and 20—error bars were smaller than the symbol size. The lower points (*blue triangles*) are found by subtracting the energy of the length $L_x/2$ system from the length L_x system and dividing by the number of extra sites of the larger system. The energy estimate $\varepsilon_0 = -0.67172(7)$ for the infinite cylinder is taken from the best subtracted data point.

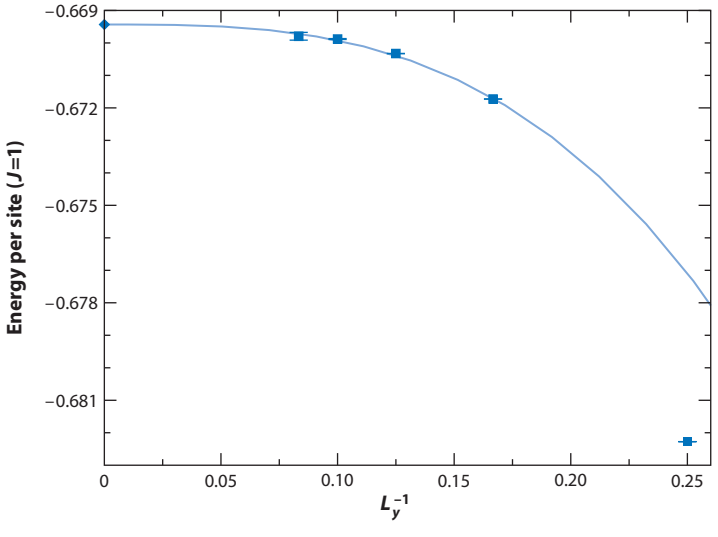

Figure 6

Extrapolation of energy estimates for infinite cylinders of the $S = 1/2$ Heisenberg model with $J = 1$. The energy densities for widths $L_y = 6$, 8, 10, and 12 are fit to a cubic polynomial $a + bL_y^{-3}$ (see Reference 74), giving an energy estimate $\varepsilon_0 = -0.6694(3)$ for the 2D system.

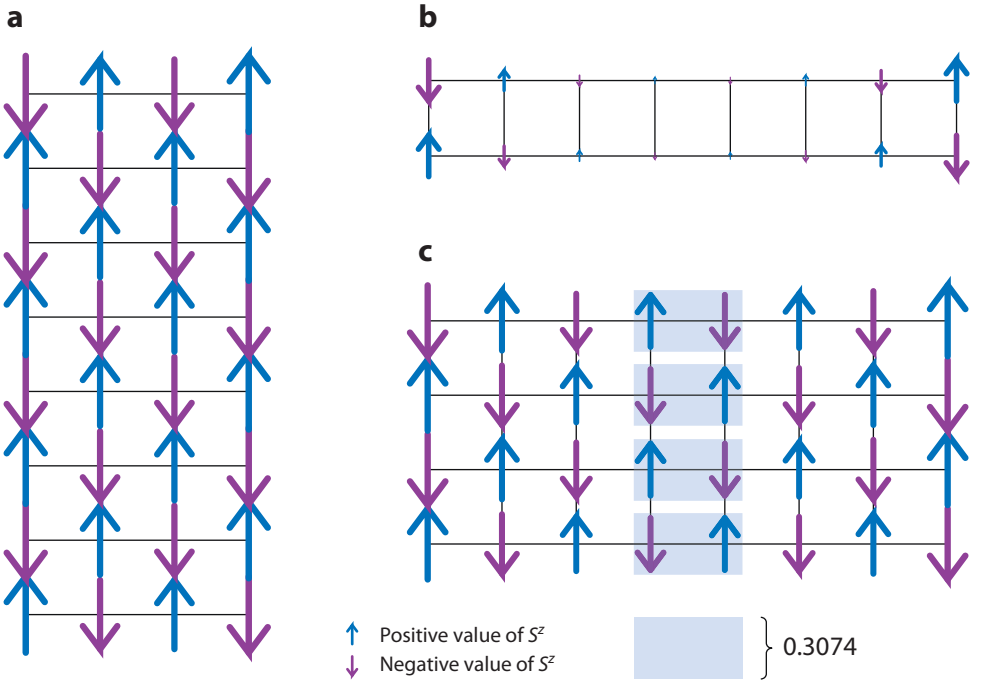

Figure 7

Ground states of the $S = 1/2$ Heisenberg model on (*a*) 4×8, (*b*) 8×2, and (*c*) 8×4 cylinders. All cylinders have a staggered pinning field of strength $J/2$ applied at the open ends. Because cylinder *a* is too short, edge effects push its bulk magnetization above the true 2D value. Cylinder *b* is too one-dimensional so its bulk magnetization falls below the 2D value. Cylinder *c* has an aspect ratio of 2:1, which is almost ideal (19), making its bulk a good approximation of the infinite 2D system. The magnetization of cylinder *c* at the center rungs ($m \simeq 0.28$) is close to the estimated 2D value of $m \simeq 0.30743$ (75).

in $1/L_y$ vanish (19). Extrapolations performed at fixed α^* will be nearly flat, improving their accuracy. For periodic boundary conditions the ideal aspect ratio turns out to be approximately $\alpha^* \simeq 7$. For cylindrical boundaries it is much lower, approximately $\alpha^* \simeq 1.9$ (19). This is yet another reason why cylindrical boundary conditions are preferred. Finite-size effects can be drastically reduced even if one does not use the exact aspect ratio.

3.3. Gaps and Excited States

In addition to ground state properties, one usually wants to have a good understanding of the elementary excitations of a system. Calculating the energy gap to the first excited state is of fundamental importance for classifying phases and estimating their robustness to perturbations. The excited states themselves can be useful for understanding subtle orders present in the ground state and for computing quantities that are accessible to experiments.

Traditionally there have been two ways to find excited states and gaps using DMRG, and both methods are a good option for studying 2D systems. The simplest situation is when an excited state lies in a different quantum number sector than the ground state. This is the case when calculating the spin gap of a magnet, for example. By taking advantage of quantum numbers, DMRG can directly target the ground state of an excited sector. This method is

preferred as long as the excitation is not attracted to the open ends of the system, which can easily be checked from measurements of local quantities. If the excitation is attracted to the ends, the restricted sweeping approach described below is a good option.

When studying excited states in the same sector as the ground state, such as singlet excitations, or when studying a model with no conserved quantities, one can simultaneously target the lowest few eigenstates. In this scheme the superblock wavefunctions for each state are kept separate but they share one set of boundary blocks. It is often necessary, therefore, to keep an increased number of states to approximate different wavefunctions using a single truncated basis.

But there are situations where neither of the above approaches is a good option. Models of topological phases often have no conserved quantities and possess a large ground state degeneracy that makes multiple targeting inefficient. For cases such as these, it is helpful to take advantage of the flexibility offered through using MPSs and matrix product operators. Representing a state as an MPS gives DMRG access to the entire wavefunction and makes it possible to compute overlaps between wavefunctions found through separate calculations.

This flexibility offers a new way to find excited states as follows. First, DMRG is used to compute a ground state $|\psi_0\rangle$ of the Hamiltonian H as an MPS. Then, one defines a Hamiltonian $H' = H + wP_0$, where $P_0 = |\psi_0\rangle\langle\psi_0|$ is a projection operator and w is an energy penalty for states not orthogonal to $|\psi_0\rangle$. If w is large enough, the ground $|\psi_1\rangle$ of H' will be the second lowest eigenstate of H (its first excited state or a second ground state).

But when finding $|\psi_1\rangle$ it is neither necessary nor advisable to compute H'. One should instead work with H and P_0 separately. During a normal Lanczos or Davidson step in DMRG, the product $H|\psi_1\rangle$ gets computed in the current local basis. The product $P_0|\psi_1\rangle$ can be computed in a similar fashion following the procedure in **Figure 8**. The resulting tensors $H|\psi_1\rangle$ and $wP_0|\psi_1\rangle$ can then be added to form $H'|\psi_1\rangle$.

Having found $|\psi_1\rangle$, one can go on to compute the next excited state by including both P_0 and $P_1 = |\psi_1\rangle\langle\psi_1|$ in the effective Hamiltonian. Many low-lying states can be found this way with a cost that is quadratic in the number of states, although the method can only be pushed so far unless the previous wavefunctions are determined to high accuracy. Finally, after finding a set of low-lying states $|\psi_n\rangle$, it is possible to obtain an even more accurate spectrum by computing the eigenvalues of $H^{m,n} = \langle\psi_m|H|\psi_n\rangle$. This last step rotates away any remaining nonorthogonality present in the states $|\psi_n\rangle$, ensuring that energies are computed in an optimal basis.

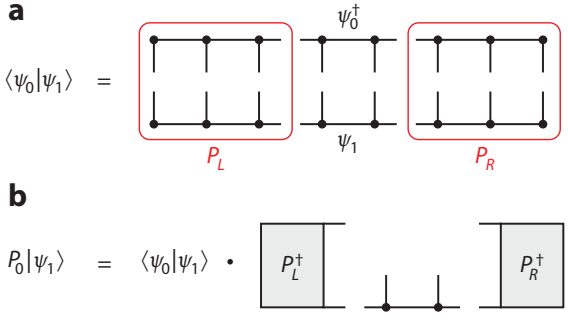

Figure 8

Steps for computing the product of a projector $P_0 = |\psi_0\rangle\langle\psi_0|$ with a state $|\psi_1\rangle$ in the density matrix renormalization group. After computing the tensors P_L and P_R that project $\langle\psi_0|$ into the current basis, one (*a*) computes the overlap $\langle\psi_0|\psi_1\rangle$ then (*b*) multiplies it by the projected form of $|\psi_0\rangle$.

Each of the three methods discussed above has its merits, but one issue that affects them all is the possibility of spurious excitations at the open ends of the cylinder. In most cases such an excitation is uninteresting given that it has no analog in the infinite 2D system. If this problem arises, one way to deal with it is through restricted sweeping. First, the ground state is computed as usual to very high accuracy. Then, within the same calculation one switches over to the first excited state either by changing quantum numbers or through multiple targeting. But now the sweeping range is restricted only to the bulk of the cylinder, keeping the system fixed to the ground state basis near the open ends. By mixing with this fixed basis, excitations can have tails extending beyond the sweeping region, but will not get stuck in an unphysical state where they live only at an edge.

4. TWO-DIMENSIONAL TENSOR NETWORK METHODS

On the basis of DMRG's success for 1D and quasi-1D systems, it is reasonable to ask if DMRG can be extended to 2D in a more natural way. Early attempts to do so failed because they did not take into account the essential differences in entanglement scaling of 1D and 2D systems. Ground states of 1D gapped Hamiltonians obey an area law: Any subsystem is entangled with its environment only through the boundary connecting the two. This means that ground states of gapped 1D systems can be represented accurately by MPS with a fixed bond dimension (21).

Most—if not all—gapped phases in 2D also obey an area law, but in 2D this means that the entanglement entropy of a subregion grows proportionally to its linear size. To capture this effect with an MPS requires that its bond dimension increase exponentially with the system size no matter how it is embedded into a 2D lattice. The key, then, to obtaining a scalable version of 2D DMRG is to identify new classes of variational wavefunctions that extend MPS to reproduce 2D area law behavior.

Though there have been several promising attempts in this direction, two classes of wavefunctions stand out based on their usefulness in simulating several realistic 2D models. The first is a natural extension of an MPS known as a projected entangled pair state or PEPS (77, 78). Just as an MPS can be viewed as a network of rank 3 tensors, a PEPS is a network of rank $Z + 1$ tensors, where Z is the coordination number of the lattice. The usefulness of PEPS is somewhat limited by the steep computational cost required to optimize them, which grows as D^{10}, where D is the bond dimension. And although a PEPS is a well-defined variational wavefunction, it is necessary to introduce approximations when computing observables, leading to energy estimates that are no longer variational. But because of the higher coordination number of 2D lattices, one expects that 2D ground states are already represented quite well by a PEPS with $D \sim 10$–100 versus an MPS for a 1D system where m must be many hundreds to achieve the same accuracy (79). Perhaps the most attractive feature of the PEPS approach is its ability to work directly in the thermodynamic limit using the so-called iPEPS method (80, 81). The iPEPS method has been successfully applied to a wide variety of models including orbital models (82), frustrated magnets (83), interacting bosons (84), and interacting fermions (85, 86).

A second type of wavefunction that has proven effective for 2D is the multiscale entanglement renormalization ansatz (MERA). Originally conceived as a concrete realization of Kadanoff's real space renormalization group, a MERA generalizes an MPS by extending the 1D chain of tensors into a layered structure where each layer represents a coarser length scale in the renormalized group process (87, 88). The MERA approach can naturally be extended to 2D by using tensors that group patches of lattice sites together instead of 1D segments. But unlike

Table 1 Comparison of some leading numerical methods for 2D strongly correlated systems

Method	Approach	Variational	2D?	Sign problem	Biased	Typical computational effort
Worldline QMC (89)	Statistical sampling	No	Yes	Yes	No	N
Determinantal QMC (13, 90)	Statistical sampling	No	Yes	Yes	No	N^3
Variational QMC (91)	Statistical sampling	Yes	Yes	Fixed by guessed wavefunction	Yes	N^3
Series expansion (92)	Extrapolated Taylor series	No	Yes	No	Yes	<10 or 20 terms
DMRG[d]	Low entanglement	Yes	Width $\lesssim$12	No	Very slight[a]	m^3
PEPS	Low entanglement	No[b]	Yes	No	Very slight[a]	D^{10}–D^{12} (P. Corboz, private communication)
MERA	Low entanglement	Yes	Yes	No	Very slight[a,c]	D^{16} (93)

[a]Indicates a bias toward states having low entanglement.
[b]Though PEPS themselves are variational, observables must be computed through a controlled approximation.
[c]The pattern of tensors chosen may favor a certain type of ground state.
[d]Abbreviations: DMRG, density matrix renormalization group; MERA, multiscale entanglement renormalization ansatz; PEPS, projected entangled pair state; QMC, quantum Monte Carlo.

the PEPS ansatz, there is no unique MERA for a given lattice. This makes the method more flexible but can also be a source of bias if the tensors are chosen to favor a certain type of ground state. MERA optimization techniques currently suffer from a higher computational cost than PEPS (see **Table 1**) but a key advantage of MERA over PEPS is that local observables may be computed exactly and efficiently, allowing MERA simulations to remain variational. This property of the MERA comes from its construction in terms of isometries that cancel outside of a "light cone" emanating from the location of the operator to be measured (88). Finally, as with the PEPS method, the MERA approach can give results for both finite systems and the thermodynamic limit. Recent applications of MERA to 2D systems include studies of interacting fermions (93), orbital systems (94), topological models (95), and frustrated magnets (28).

A key question is this: When should one use 2D DMRG methods, and when should one try PEPS or MERA (or another approach)? As a first step in addressing this issue, we provide in **Figure 9** a simple comparison between iPEPS results (P. Corboz, private communication) and DMRG data for the 2D square lattice Heisenberg model. (We hope that comparable data for MERA can be provided in the future.) The accuracy of iPEPS depends on the tensor dimension D, whereas that of DMRG depends on m and the width of the cylinder studied. At some width, which depends on how large an m or D can be treated with current computing resources, DMRG becomes less accurate than iPEPS. (Neither the values of m nor of D shown in the figure should be thought of as reflecting the state of the art.) Whether one should use DMRG or iPEPS depends primarily on whether the bulk behavior can be extrapolated with cylinders smaller than this width. Alternatively, it can be very useful to use both DMRG and iPEPS or MERA, and compare results.

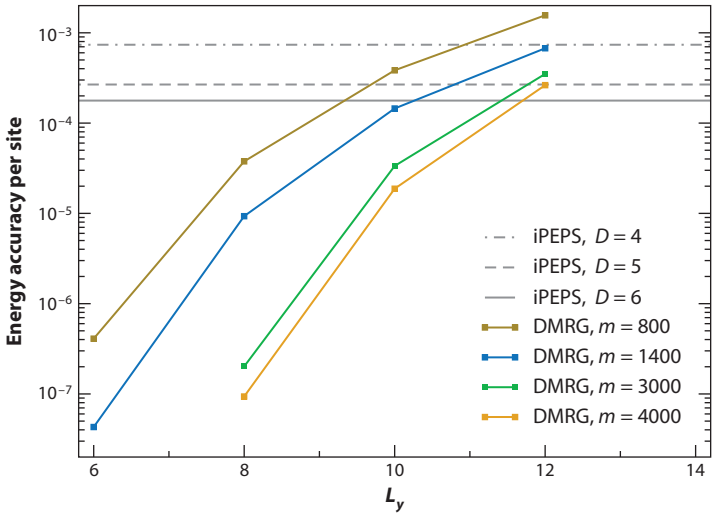

Figure 9

Plots of the accuracy achievable with DMRG for cylinders of width L_y and a maximum number of states kept m. Data are for the $S = 1/2$ square lattice Heisenberg model with $J = 1$. The DMRG accuracy is defined as the difference between the energy for a fixed m and the energy obtained by extrapolating in the truncation error. The horizontal lines show the difference between iPEPS energy estimates (P. Corboz, private communication) and the QMC estimate $\varepsilon_0 = -0.669437(5)$ (75). Because one is always restricted to some maximum m in DMRG, it is only worthwhile to extrapolate using widths L_y for which there is a better accuracy than iPEPS; for simulations of larger systems it is more sensible to use PEPS or MERA directly. Abbreviations: DMRG, density matrix renormalization group; MERA, multiscale entanglement renormalization ansatz; PEPS, projected entangled pair state; QMC, quantum Monte Carlo.

DISCLOSURE STATEMENT

The authors are not aware of any affiliations, memberships, funding, or financial holdings that might be perceived as affecting the objectivity of this review.

ACKNOWLEDGMENTS

We acknowledge helpful discussions with Sasha Chernyshev; Salvatore Manmana; and Philippe Corboz, who was kind enough to provide iPEPS data for the square lattice Heisenberg model. We acknowledge support from the NSF under DMR-0907500.

LITERATURE CITED

1. Bergman D, Alicea J, Gull E, Trebst S, Balents L. 2007. *Nat. Phys.* 3:487–91
2. Castelnovo C, Moessner R, Sondhi S. 2008. *Nature* 451:42–45
3. Dagotto E. 1994. *Rev. Mod. Phys.* 66:763–840
4. Kastner MA, Birgeneau RJ, Shirane G, Endoh Y. 1998. *Rev. Mod. Phys.* 70:897–928
5. Stormer HL, Tsui DC, Gossard AC. 1999. *Rev. Mod. Phys.* 71:S298–305
6. Balents L. 2010. *Nature* 464:199–208
7. Yamashita M, Nakata N, Kasahara Y, Sasaki T, Yoneyama N, et al. 2009. *Nat. Phys.* 5:44–47
8. Yamashita M, Nakata N, Senshu Y, Nagata M, Yamamoto HM, et al. 2010. *Science* 328:1246–48
9. Yan S, Huse DA, White SR. 2011. *Science* 332:1173–76

10. Giamarchi T. 2003. *Quantum Physics in One Dimension*. Oxford, UK: Oxford Univ. Press
11. Sandvik AW. 2007. *Phys. Rev. Lett.* 98:227202
12. Isakov SV, Hastings MB, Melko RG. 2011. *Nat. Phys.* 7:772–75
13. White SR, Scalapino DJ, Sugar RL, Loh EY, Gubernatis JE, Scalettar RT. 1989. *Phys. Rev. B* 40:506–16
14. Troyer M, Wiese UJ. 2005. *Phys. Rev. Lett.* 94:170201
15. White SR. 1992. *Phys. Rev. Lett.* 69:2863–66
16. White S. 1993. *Phys. Rev. B* 48:10345–56
17. Lüscher A, Läuchli AM. 2009. *Phys. Rev. B* 79:195102
18. Poilblanc D, Mambrini M, Schwandt D. 2010. *Phys. Rev. B* 81:180402R
19. White SR, Chernyshev A. 2007. *Phys. Rev. Lett.* 99:127004
20. Schollwöck U. 2005. *Rev. Mod. Phys.* 77:259–315
21. Hastings MB. 2007. *J. Stat. Mech.* 2007:P08024
22. White S, Huse D. 1993. *Phys. Rev. B* 48:3844–52
23. Schollwöck U, White SR. 2006. arxiv:cond-mat/0606018
24. White SR. 2009. *Phys. Rev. Lett.* 102:190601
25. Stoudenmire E, White SR. 2010. *N. J. Phys.* 12:055026
26. Östlund S, Rommer S. 1995. *Phys. Rev. Lett.* 75:3537–40
27. Jiang HC, Weng ZY, Xiang T. 2008. *Phys. Rev. Lett.* 101:090603
28. Evenbly G, Vidal G. 2010. *Phys. Rev. Lett.* 104:187203
29. Wang L, Pižorn I, Verstraete F. 2011. *Phys. Rev. B* 83:134421
30. McCulloch I. 2008. arxiv:0804.2509
31. Kallin AB, Hastings MB, Melko RG, Singh RRP. 2011. arxiv:1107.2840
32. Schollwöck U. 2011. *Ann. Phys.* 326:96–192
33. Hallberg KA. 2006. *Adv. Phys.* 55:477–526
34. Noack RM, Manmana SR. 2005. *AIP Conf. Proc.* 789:93–163
35. White SR. 1996. *Phys. Rev. Lett.* 77:3633–36
36. Yoshikawa S, Okunishi K, Senda M, Miyashita S. 2004. *J. Phys. Soc. Jpn.* 73:1798–804
37. Weng M, Sheng DN, Weng ZY, Bursill RJ. 2006. *Phys. Rev. B* 74:012407
38. Jiang HC, Weng ZY, Sheng DN. 2008. *Phys. Rev. Lett.* 101:117203
39. Capriotti L, Scalapino DJ, White SR. 2004. *Phys. Rev. B* 93:177004
40. Jiang HC, Krüger F, Moore JE, Sheng DN, Zaanen J, Weng ZY. 2009. *Phys. Rev. B* 79:174409
41. Sheng DN, Motrunich OI, Fisher MPA. 2009. *Phys. Rev. B* 79:205112
42. Block MS, Sheng DN, Motrunich OI, Fisher MPA. 2011. *Phys. Rev. Lett.* 106:157202
43. Jiang HC, Gu ZC, Qi XL, Trebst S. 2011. *Phys. Rev. B* 83:245104
44. White SR, Noack RM, Scalapino DJ. 1994. *Phys. Rev. Lett.* 73:886–89
45. du Croo de Jongh M, van Leeuwen J. 1998. *Phys. Rev. B* 57:8494–500
46. Zhao J, Wang X, Xiang T, Su Z, Yu L, et al. 2006. *Phys. Rev. B* 73:012411
47. White SR, Scalapino DJ. 1997. *Phys. Rev. B* 55:R14701–4
48. White SR, Scalapino DJ. 1998. *Phys. Rev. Lett.* 80:1272–75
49. White SR, Scalapino DJ. 1998. *Phys. Rev. Lett.* 81:3227–30
50. Tohyama T, Gazza C, Shih CT, Chen YC, Lee TK, et al. 1999. *Phys. Rev. B* 59:R11649–52
51. White SR, Scalapino DJ. 1999. *Phys. Rev. B* 60:R753–56
52. Kampf AP, Scalapino DJ, White SR. 2001. *Phys. Rev. B* 64:052509
53. Emery VJ, Kivelson SA, Lin HQ. 1990. *Phys. Rev. Lett.* 64:475–78
54. White SR, Scalapino DJ. 2000. *Phys. Rev. B* 61:6320–26
55. Scalapino DJ, White SR. 2001. *Found. Phys.* 31:27–39
56. Chernyshev AL, White SR, Neto AHC. 2002. *Physica B* 312–13:566–68
57. Chernyshev AL, White SR, Castro Neto AH. 2002. *Phys. Rev. B* 65:214527
58. White SR, Scalapino DJ. 2004. *Phys. Rev. B* 70:220506R
59. Chernyshev AL, Castro Neto AH, White SR. 2005. *Phys. Rev. Lett.* 94:036407
60. White SR, Scalapino DJ. 2009. *Phys. Rev. B* 79:220504
61. White SR, Scalapino DJ. 2003. *Phys. Rev. Lett.* 91:136403

62. Hager G, Wellein G, Jeckelmann E, Fehske H. 2005. *Phys. Rev. B* 71:075108
63. Fehske H, Hager G, Wellein G, Jeckelmann E. 2006. *Physica B* 378–80:319–20
64. Jiang HC, Weng M, Weng ZY, Sheng DN, Balents L. 2009. *Phys. Rev. B* 79:020409R
65. Motrunich OI, Fisher MPA. 2007. *Phys. Rev. B* 75:235116
66. Sheng DN, Motrunich OI, Trebst S, Gull E, Fisher MPA. 2008. *Phys. Rev. B* 78:054520
67. Block MS, Mishmash RV, Kaul RK, Sheng DN, Motrunich OI, Fisher MPA. 2011. *Phys. Rev. Lett.*
68. Feiguin AE, Fisher MPA. 2011. *Phys. Rev. B* 83:115104
69. Nishimoto S, Nakamura M, O'Brien A, Fulde P. 2010. *Phys. Rev. Lett.* 104:196401
70. Jeckelmann E, White SR. 1998. *Phys. Rev. B* 57:6376–85
71. Liang S, Pang H. 1994. *Phys. Rev. B* 49:9214–17
72. Dukelsky J, Martin-Delgado MA, Nishino T, Sierra G. 1998. *Europhys. Lett.* 43:457–62
73. White SR. 2005. *Phys. Rev. B* 72:180403
74. Neuberger H, Ziman T. 1989. *Phys. Rev. B* 39:2608–18
75. Sandvik AW. 1997. *Phys. Rev. B* 56:11678–90
76. Sandvik AW, Evertz HG. 2010. *Phys. Rev. B* 82:024407
77. Nishino T, Hieida Y, Okunishi K, Maeshima N, Akutsu Y, Gendiar A. 2001. *Prog. Theor. Phys.* 105:409–17
78. Verstraete F, Porras D, Cirac JI. 2004. *Phys. Rev. Lett.* 93:227205
79. Verstraete F, Murg V, Cirac JI. 2008. *Adv. Phys.* 57:143–224
80. Jordan J, Orús R, Vidal G, Verstraete F, Cirac JI. 2008. *Phys. Rev. Lett.* 101:250602
81. Orús R, Vidal G. 2009. *Phys. Rev. B* 80:094403
82. Orús R, Doherty AC, Vidal G. 2009. *Phys. Rev. Lett.* 102:077203
83. Bauer B, Vidal G, Troyer M. 2009. *J. Stat. Mech.* 2009:P09006
84. Jordan J, Orús R, Vidal G. 2009. *Phys. Rev. B* 79:174515
85. Corboz P, Orús R, Bauer B, Vidal G. 2010. *Phys. Rev. B* 81:165104
86. Corboz P, Jordan J, Vidal G. 2010. *Phys. Rev. B* 82:245119
87. Vidal G. 2007. *Phys. Rev. Lett.* 99:220405
88. Evenbly G, Vidal G. 2009. *Phys. Rev. B* 79:144108
89. Sandvik AW. 2010. *AIP Conf. Proc.* 1297:135–338
90. Blankenbecler R, Scalapino DJ, Sugar RL. 1981. *Phys. Rev. D* 24:2278–86
91. Foulkes WMC, Mitas L, Needs RJ, Rajagopal G. 2001. *Rev. Mod. Phys.* 73:33–83
92. Domb C, Green M. 1974. *Phase Transitions and Critical Phenomena*, *Vol. 3*. London: Academic
93. Corboz P, Evenbly G, Verstraete F, Vidal G. 2010. *Phys. Rev. A* 81:010303
94. Cincio L, Dziarmaga J, Oleś AM. 2010. *Phys. Rev. B* 82:104416
95. Tagliacozzo L, Vidal G. 2011. *Phys. Rev. B* 83:115127

Annual Review of
Condensed Matter
Physics

Volume 3, 2012

Contents

Errata

An online log of corrections to *Annual Review of Condensed Matter Physics* articles may be found at http://conmatphys.annualreviews.org/errata.shtml